Effect of nickel contamination on high carrier lifetime *n*-type crystalline silicon

Yohan Yoon,[1,a)] Bijaya Paudyal,[2] Jinwoo Kim,[1] Young-Woo Ok,[3] Prashant Kulshreshtha,[4] Steve Johnston,[5] and George Rozgonyi[1]
[1]*Department of Materials Science and Engineering, North Carolina State University, Raleigh, North Carolina 27695, USA*
[2]*MKS Instruments Inc, 134 Rio Robels Drive, San Jose, California 95134, USA*
[3]*University Center of Excellence for Photovoltaics Research and Education, School of Electrical and Computer Engineering, Georgia Institute of Technology, Atlanta, Georgia 30332-0250, USA*
[4]*Lawrence Berkeley National Laboratory, MS-67R2206, 1 Cyclotron Road, Berkeley, California 94720, USA*
[5]*National Renewable Energy Laboratory, 1617 Cole Blvd., Golden, Colorado 80401, USA*

(Received 6 December 2011; accepted 14 December 2011; published online 2 February 2012; publisher error corrected 6 February 2012)

The injection-dependent lifetimes of different levels of Ni-contaminated *n*-type Czochralski (CZ) silicon wafers were investigated using resonant-coupled photoconductance decay (RCPCD) and quasi-steady-state photoconductance technique (QSSPC). The lifetime degradation of the most heavily contaminated samples was caused by Ni silicide precipitates at the surface of the wafers. The impact on lifetime was determined by surface recombination velocities (*SRV*). *SRV* values from RCPCD were comparable to those extracted by the QSSPC technique. A direct correlation between minority carrier lifetime and the concentration of electrically active substitutional Ni and Ni silicide precipitate traps measured using deep level transient spectroscopy was established. © *2012 American Institute of Physics*. [doi:10.1063/1.3680880]

INTRODUCTION

The detrimental effects and electrical properties of transition-metal impurities, e.g., iron and its complexes, such as FeB, in *p*-type silicon are well-known.[1] However, in *n*-type silicon wafers, the impact of specific metallic impurities on minority lifetimes is not as well established. Nickel is one of the main impurities, which can contaminate the wafer during the solar cell manufacturing process.[2] Due to its high diffusivity, nickel can form precipitates at the wafer surface or decorate existing lattice defects.[3,4] These band-like defects act as recombination centers and decrease the effective lifetime.[5] Surface recombination velocity (*SRV*) is useful to evaluate the impact of precipitates at the surface of wafers.[6] *SRV* and injection-level–dependent lifetimes have been determined using quasi-steady-state photoconductance technique (QSSPC)[5,7] and microwave-detected photoconductance decay (MWPCD).[8,9] However, for more accurate calculation, the studies about the separation of bulk and surface components of effective lifetimes[10] are still in demand. In this paper, the method for the separation of bulk and surface component of recombination is suggested by RCPCD signal transient, and measured *SRV* is verified against the extracted *SRV* from QSSPC measurements.

Shockley-Read-Hall (SRH) recombination[11,12] is affected by electrically active impurities or traps. Ni-related electrically active defects[13,14] and precipitates[15] have been measured using deep level transient spectroscopy (DLTS) by a number of authors in the past. However, the fraction of electrically active defects of Ni-contaminated samples following a high temperature diffusion is on the order of 10^{-3} to 10^{-4} that of the total Ni in the silicon sample.[16] Rapid quenching after a high temperature annealing may slightly increase the ratio.[17] For this reason, Ni-related deep-level impurities have been mostly negligible and ignored in the past. However, in high purity wafers, even a small concentration ($<10^{12}\,cm^{-3}$) of impurities can cause a significant degradation in minority carrier lifetime. In this study, Ni-related electrically active defects in samples with different low levels of Ni-contamination were examined using DLTS and compared with lifetime data.

EXPERIMENTAL

High lifetime (2.9 ms), six-inch diameter, 5 Ω·cm phosphorus–doped ($9.2 \times 10^{14}\,cm^{-3}$ *n*-type), 200-μm-thick Czochralski (CZ) silicon wafers were selected for Ni contamination. For comparison, a control wafer was not contaminated and annealed. The wafers were RCA cleaned (a recipe developed by the RCA (Radio Corporation of America)) before dipping into a Ni-spiked solution (1 mg/ml) at room temperature. A 30-min, 575 °C to 770 °C drive-in annealing was then performed in a vertical tube furnace under Argon (Ar) ambient, followed by slow cooling in air. Four levels of Ni contamination (labeled N1 to N4) were obtained (see Table I). The total Ni concentrations of the four samples were measured by inductively coupled plasma mass spectrometry (ICP-MS). Note that the Ni concentrations are average values of the 200 μm samples and only qualitatively reflect the near-surface concentrations where the electrical analyses were performed.

To evaluate the surface recombination component of the contaminated samples, N1 to N4 were etched in a 20% KOH: 80% H_2O solution, which removed ~ 5 μm from the

a)Author to whom correspondence should be addressed. Electronic mail: yyoon3@ncsu.edu.

TABLE I. Drive-in annealing temperature and averaged ICP-MS concentrations of Ni-contaminated phosphorus doped to 9.2×10^{14}, 5 Ω cm, n-type CZ samples

Sample identification	Annealing temperature (°C)	Ni concentration measured by ICP-MS ($\times 10^{12}\,cm^{-3}$)
N1	575	5.2
N2	634	9.3
N3	712	25
N4	769	62

surface. Minority carrier lifetimes were measured using QSSPC and RCPCD with the samples immersed in an iodine-ethanol solution during the lifetime measurements for surface passivation. The QSSPC technique determines the minority carrier lifetimes as a function of excess carrier concentration, Δn. Injection-dependent lifetime spectroscopy (IDLS)[18] was used in order to probe deeper into the electrical properties of Ni impurities in Si at various injection levels. The recombination properties of these Ni-contaminated samples were compared at the same injection level, $\eta = \Delta n/N_{dop}$, where N_{dop} is the phosphorus doping concentration. Resonant-coupled photoconductance decay (RCPCD), a transient-based technique for obtaining lifetimes from photoconductivity decay curves as a function of time, was used next. A Nd:YAG laser with an optical parametric oscillator provides carrier excitation in the form of $3 \sim 5$ ns pulses of 1000 nm wavelength light. The RCPCD system measures photoconductivity by inductive-coupling of a coil to the wafer using approximately 420 MHz. Finally, a Bio-Rad DL8000 system DLTS was used to determine the concentration and trap energy of electrically active defects in the contaminated samples. Evaporated gold Schottky diode DLTS measurements were carried out at −3 V reverse biased and pulsed at 3.2 V for 100 μs.

RESULTS AND DISCUSSION

Figure 1(a) plots the QSSPC-determined room temperature effective lifetime (τ_{eff}) of four Ni-contaminated plus one uncontaminated reference *n*-type Si wafer. At the injection level of phosphorus doping density ($9 \times 10^{14}\,cm^{-3}$), $\eta = 1$, the effective lifetimes of N1, N2, and N3 gradually decrease with increasing Ni concentration and are not greatly different from each other; however, sample N4, which has the highest contamination level, is significantly lower. Note that, for the etched samples (see Fig. 1(b)), the effective lifetime of sample N4-E is noticeably higher than, not only non-etched sample N4, but even other etched samples N2-E and N3-E. It appears that, at the highest Ni contamination level of sample N4 ($6.2 \times 10^{13}\,cm^{-3}$), localized surface recombination centers are formed, which seriously decrease the lifetime at the sample surface, but apparently are dissolved out during the etching process. It is well known that Ni, particularly interstitial Ni (Ni_i) has high diffusivity in silicon (2.5×10^{-11} cm^2/s at RT).[2] The majority of dissolved Ni_i diffuses to the sample surface during the cooling process in the air after drive-in annealing. Therefore, at the surface Ni, concentrations beyond the solid solubility limit are likely to form precipitates.[2]

The presence of Ni precipitates can be inferred by *SRV* (cm/s) and extracted from the expression

$$1/\tau_{eff} = 1/\tau_b + 2S/W \quad (1)$$

(where τ_b is the bulk lifetime, W the wafer thickness, and S the surface recombination velocity).

The *SRV* values are essential in separating the bulk lifetime as measured by the effective lifetime after the surface-etching process. However, the effective lifetime of etched samples may not correspond to the true bulk lifetime, since some precipitates or stress-induced dislocations may still exist in the bulk after the shallow etching process. Therefore, the separation of surface recombination and bulk recombination is

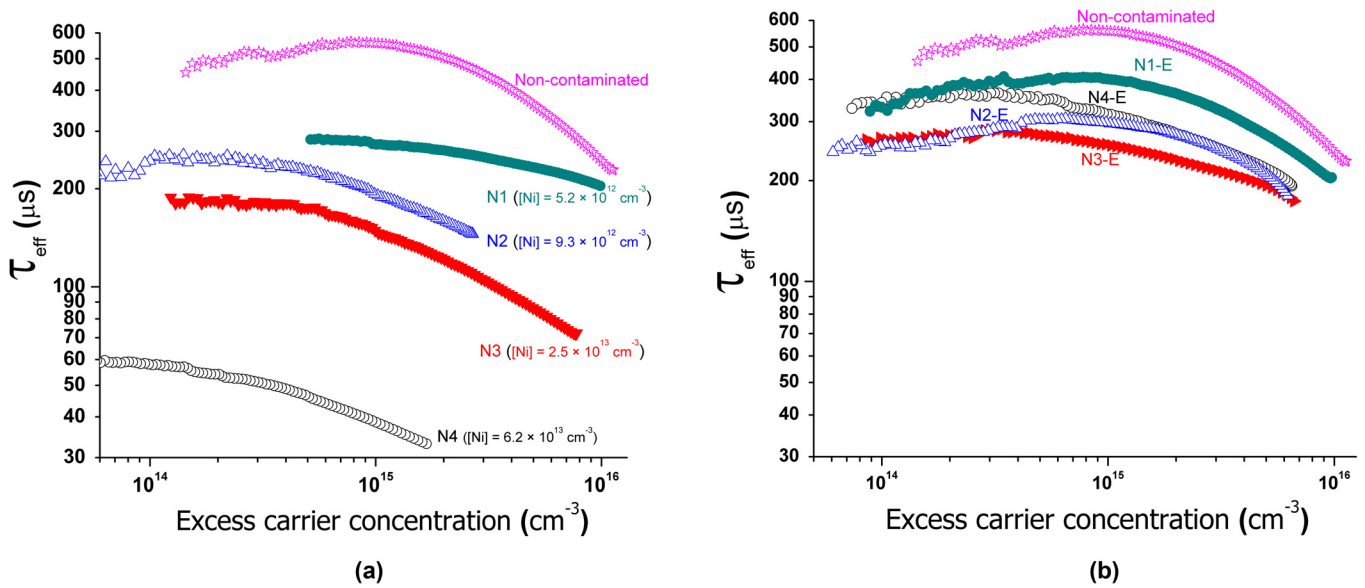

FIG. 1. (Color online) Effective carrier lifetime (τ_{eff}) as a function of excess carrier concentration (Δn) for (a) non-etched (b) etched (5 μm removed both surfaces) n-type CZ samples with various Ni concentrations.

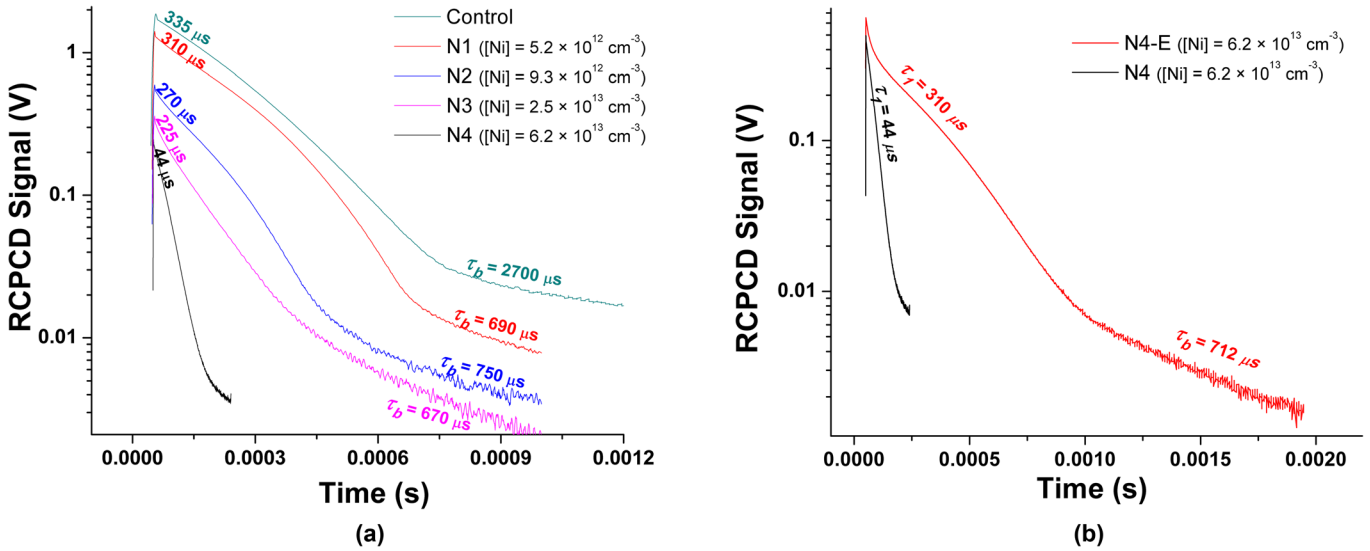

FIG. 2. (Color online) RCPCD signal as a function of time for (a) control (non-contaminated) sample and different levels of Ni-contaminated samples and (b) the comparison of non-etched N4 sample and etched N4 sample (N4-E).

needed and was carried out using RCPCD injection-dependent lifetime data.

Figure 2 shows the RCPCD signal as a function of time for the Ni-contaminated samples N1 to N4, the control sample, and etched N4-E sample. Each sample has a transient with two or three different slopes, as a result of a varying balance of recombination mechanisms. The slope of the transient curve has been converted to lifetime by the following equation:

$$\Delta p(t) = \Delta p_o e^{(-t/\tau)} \tag{2}$$

(where τ is the lifetime. The lifetime is then obtained by plotting $ln[\Delta p(t)]$ versus time and measuring the slope of the plot.).

The initial instantaneous lifetime at t = 0 is[19]

$$\tau_1 = \tau_B/(1 + \alpha S \tau_B) \tag{3}$$

(where τ_B is the bulk lifetime and α the absorption coefficient).

When the initial lifetime is much shorter than the bulk lifetime,

$$\tau_1 = 1/\alpha S, \tag{4}$$

the initial lifetime is dominated by surface recombination.

The bulk lifetime is then determined according to the relationship

$$1/\tau_B = 1/\tau_{SRH} + 1/\tau_{rad} + 1/\tau_{Auger}, \tag{5}$$

where τ_{SRH} is the Shockley-Read-Hall recombination, τ_{rad} the radiative recombination, and τ_{Auger} the Auger recombination.

At low injection levels ($\eta < 1$), τ_{rad} and τ_{Auger} are much longer than τ_{SRH}. Therefore, bulk lifetime is expressed by[20]

$$1/\tau_B \approx 1/\tau_{SRH} = \left(1 + (C/C_{ref})\right)/\tau_{max}, \tag{6}$$

where τ_{max} is the low-injection SRH lifetime (lifetime of a second slope), C the doping concentration, and C_{ref} an experimentally determined constant ($7 \times 10^{15}\,cm^{-3}$).

In this study, τ_B is 1.13 τ_{max} from Eq. (6) and the bulk lifetime component of the control sample (see Fig. 2(b)) is 2.7 ms, well matched with the 2.9 ms lifetime measured for the silicon ingot before wafer slicing, for which surface recombination is not an issue. This demonstrates that the bulk lifetime corresponds to the second slope in Fig. 2.

The strong surface recombination of sample N4 at high injection levels produces a much shorter lifetime, 44 μs, than other contaminated samples, but improved to 310 μs following etching (see Fig. 2). This is well matched with the QSSPC data (see Fig. 1). Note that the bulk lifetime of N4 ($\sim$ 210 μs) is not accurate, since the second slope is not linear, due to the RCPCD signal initially decaying so

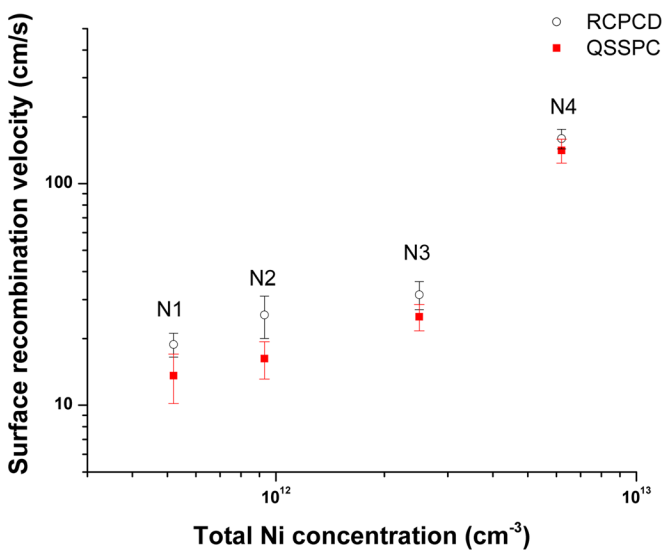

FIG. 3. (Color online) Surface recombination velocity (*SRV*) calculated by QSSPC and RCPCD as a function of total Ni concentration at a fixed injection level of $\eta = 1$.

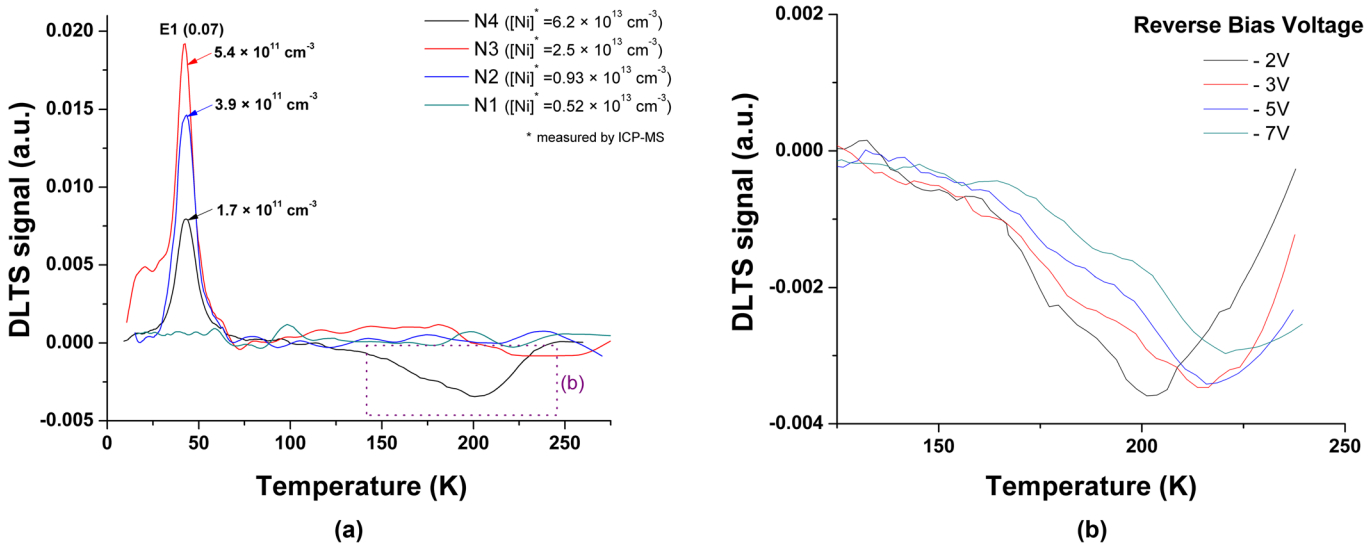

FIG. 4. (Color online) DLTS spectra for (a) a set of surface-etched, Ni-contaminated, high lifetime, n-type CZ samples with both sharp, fixed position, and Ni_s-positive trap peaks, and (b) one broad negative mobile with various reverse bias voltage from −2 V to −7 V extended defect peak for etched sample N4.

strongly that the second slope could not be saturated. Thus, the bulk lifetime of N4-E can be used for N4.

Figure 3 shows the surface recombination velocity as a function of total Ni concentration using QSSPC and RCPCD. The surface recombination velocities at the fixed injection level of $\eta = 1$ for QSSPC measurement were extracted by Eq. (1). Also, τ_B and τ_{eff} are replaced by $1.13 \times \tau_{max}$ and τ_1, respectively, for RCPCD measurement. The surface recombination velocity of RCPCD is comparable to that of QSSPC. Note that *SRV* values of RCPCD are slightly higher than that of QSSPC, since the effect of remaining precipitates at the surface of the etched sample can be removed in the case of RCPCD.

The lifetime shapes of N3-E and N4-E at a low injection level ($\eta < 1$), which is mostly affected by SRH recombination, are different to those of N1-E and N2-E samples (see Fig. 1(b)). Also, the bulk lifetime of the N4-E is still lower than the bulk lifetime of the control sample (see Fig. 2(b)). It means that some electrically active defects exist in the bulk.

Figure 4 shows DLTS spectra for etched, Ni-contaminated samples. However, non-etched samples could not be measured, since shallow polishing is needed to improve the electrical performance of the evaporated Schottky contacts and minimize the leakage current. The electron trap E1 at 45 K is attributed to the substitutional Ni double acceptor[2] and is present in most of the contaminated samples, except for the control sample and the most lightly contaminated sample N1-E, which had no signal detected above the DLTS detection limit ($1 \times 10^{11}\,cm^{-3}$). The activation energy and capture cross-sections for E1 are 0.07 eV and $3.22 \times 10^{-18}\,cm^2$, respectively. As the Ni concentration increases, the concentration of trap E1 increased (trap densities of N2-E and N3-E are $3.9 \times 10^{11}\,cm^{-3}$ and $5.4 \times 10^{11}\,cm^{-3}$, respectively), since the substitutional Ni cannot reach the wafer surface and precipitates due to its low diffusivity.[2] However, the concentration of trap E1 for the most heavily contaminated sample N4-E ($1.7 \times 10^{11}\,cm^{-3}$) decreases compared to N2-E and N3-E and, in addition, exhibits a broad negative peak from 150 ∼ 250 K. This broad peak was examined with various reverse bias voltages, which change space charge sampling regions, and the peak position shift with reverse bias voltage suggests that this peak is due to extended defects, such as Ni precipitates[15] or associated dislocations, since nickel can precipitate locally during cooling due to its low solubility at low temperatures. These precipitates and deep level impurities are responsible for the different recombination properties observed in the bulk (see Fig. 2).

In conclusion, the impact of Ni on high carrier lifetime is mainly limited to wafer surfaces when the concentration exceeds the certain level. The lifetime degradation can be recovered by a few μm etching, even though substitutional Ni and small Ni precipitates still remain in the bulk and affect effective lifetime. The SRV extracted from RCPCD measurements is very useful in separating surface and bulk recombination mechanisms, allowing the improvement of lifetime by shallow etching to be quantitatively tracked. The distribution of electrically active defects or traps as recombination sites depends on the thermal conditions and diffusivity of metallic impurities. Other transition metals, such as Mo and Ti, which have relatively low diffusivity, tend to form moderate concentrations of interstitial centers at room temperature after high temperature processing. Further studies about the effect of these transition metals (below Group 8 in the periodic table)[21] are continuing.

[1]D. Macdonald, T. Roth, P. N. K. Deenapanray, T. Trupke, and R. A. Bardos, Appl. Phys. Lett. **89**, 142107 (2006).
[2]K. Graff, *Metal Impurities in Silicon Device Fabrication*, Springer Series in Materials Science, 2nd ed. (Springer-Verlag, Berlin, 2000).
[3]M. Hourai, K. Murakami, T. Shigematsu, N. Fujino, and T. Shiraiwa, Jpn. J. Appl. Phys. **28**, 2413 (1988).
[4]M. B. Shabani, T. Yoshimi, S. Okuuchi, and H. Abe, Solid State Phenom. **57–58**, 81 (1997).
[5]D. Macdonald, Appl. Phys. A **81**, 1619 (2005).
[6]M. L. Polignano, F. Cazzaniga, A. Sabbadini, G. Queirolo, A. Cacciato, and A. D. Bartolo, Mater. Sci. Eng., B **42**, 157 (1996).

[7]R. Sinton, A. Cuevas, and M. Stuckings, in *Proceedings of the 25th IEEE Photovoltaic Specialists Conference (PVSC)*, Washington, DC, 13–17 May 1996, p. 547.
[8]S. Eranen and M. Blomberg, J. Appl. Phys. **56**, 8 (1984).
[9]J. Schmidt and A. G. Aberle, J. Appl. Phys. **81**, 9 (1997).
[10]A. Buczkowski, Z. J. Radzimski, G. A. Rozgonyi, and F. Shimura, J. Appl. Phys. **72**, 7 (1992).
[11]W. Shockley and W. T. Read, Phys. Rev. **87**, 835 (1952).
[12]R. N. Hall, Phys. Rev. **87**, 387 (1952).
[13]M. Shiraishi, J. U. Sachse, H. Lemke, and J. Weber, Mater. Sci. Eng., B **58**, 130 (1999).
[14]H. Kitagawa, S. Tanaka, H. Nakashima, and M. Yoshida, J. Electron. Mater. **20**, 461 (1991).
[15]W. Schröter, J. Kronewitz, U. Gnauert, F. Riedel, and M. Seibt, Phys. Rev. B **52**, 13726 (1995).
[16]A. A. Istratov and E. R. Weber, Appl. Phys. A: Mater. Sci. Process. **66**, 123 (1998).
[17]H. Indusekhar and V. Kumar, J. Appl. Phys. **61**, 1449 (1987).
[18]J. E. Birkholz, K. Bothe, D. Macdonald, and J. Schmidt, J. Appl. Phys. **97**, 103708 (2005).
[19]R. K. Ahrenkiel and S. W. Johnston, Sol. Energy Mater. Sol. Cells **93**, 645 (2009).
[20]A. W. Stephens, A. G. Aberle, and M. A. Green, J. Appl. Phys. **76**, 363 (1994).
[21]D. Macdonald and L. J. Geerligs, Appl. Phys. Lett. **85**, 4061 (2004).